

Limit Surfaces of Riemann Examples

David Hoffman, Wayne Rossman

1 Introduction

The only connected minimal surfaces foliated by circles and lines are domains on one of the following surfaces: the helicoid, the catenoid, the plane, and the examples of Riemann ([Ri] p329-33, [En] p403-6, [Ni] p85-6). All these surfaces are complete and embedded. Topologically they are planar domains: the helicoid is simply-connected, the catenoid is an annulus (conformally a twice-punctured sphere), and each Riemann example (see Figure 1) is conformal to the plane minus the points $\{(n,0), (\frac{1}{n},0) \mid n \in \mathbb{Z}\}$ [HKR]. In this section we will show that the plane, helicoid, and catenoid arise naturally as limits of well-chosen and properly normalized sequences of Riemann examples. The local behavior of domains on Riemann examples accounts for the existence of these limits, thus allowing a change of topology in the limit surfaces.

Theorem 1.1 *Any sequence of Riemann examples that converges to a surface in \mathbb{R}^3 converges either to a Riemann example, a helicoid, a catenoid, an infinite set of equally spaced parallel planes, or a single plane. Furthermore, there exist sequences of Riemann examples that converge to each of these possibilities.*

In order to be precise, we state what we mean by convergence of surfaces in \mathbb{R}^3 in this context.

Definition 1.1 *A sequence of surfaces $\{\mathcal{S}_i\}_{i=1}^\infty$ converges as $i \rightarrow \infty$ to a surface \mathcal{S} in \mathbb{R}^3 if, for any compact region $B \subseteq \mathbb{R}^3$, there exists an integer N_B such that for $i > N_B$, $\mathcal{S}_i \cap B$ is a normal graph over \mathcal{S} , and $\{\mathcal{S}_i \cap B\}_{i=N_B}^\infty$ converges to \mathcal{S} in the C^∞ -topology.*

One can define analogously the convergence of a one-parameter family $\mathcal{S}_t, t \in \mathbb{R}$, as $t \rightarrow t_0$. Since this convergence is in the C^∞ -topology, it requires that derivatives of all orders of the coordinate functions on the graphs converge to the corresponding derivatives of the coordinate functions on the limit-surface.

We observe that catenoids, helicoids, and planes are limit-surfaces of sequences of Riemann examples. Therefore the collection of connected embedded minimal surfaces foliated by circles and lines is itself connected in the topology associated with this convergence.

We wish to thank Rob Kusner, Pascal Romon, Ed Thayer, Johannes Nitsche and Harold Rosenberg for helpful conversations.

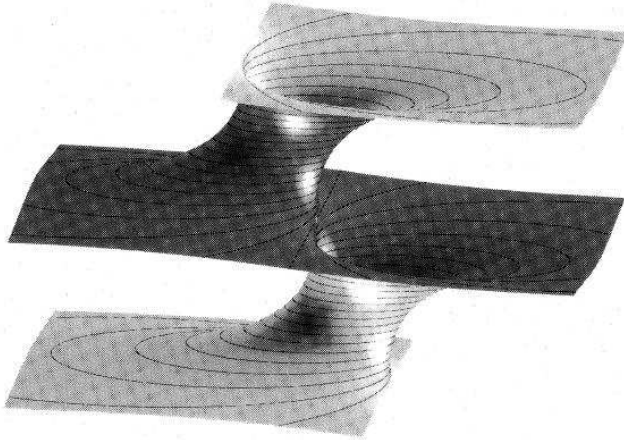


Figure 1: The Riemann Example \mathcal{R}_λ , $\lambda = 1$

2 The Family of Riemann Examples

2.1 Definition of the Riemann Examples

We now describe properties of the Riemann examples, and we give a Weierstrass representation for these surfaces. Proofs of the statements in this section may be found in [HKR].

For any Riemann example \mathcal{R} , there exists a translation T of \mathbb{R}^3 so that T : leaves \mathcal{R} invariant; is orientation-preserving on \mathcal{R} ; generates the full cyclic orientation-preserving translation symmetry group of \mathcal{R} . The quotient-surface \mathcal{R}/T is a twice-punctured rectangular torus. Thus, Riemann examples can be parametrized via a Weierstrass representation on such a torus. Fix $\lambda > 0$. We first define \bar{M}_λ :

$$\bar{M}_\lambda = \left\{ (z, w) \in (\mathbb{C} \cup \{\infty\})^2 : w^2 = z(z - \lambda)\left(z + \frac{1}{\lambda}\right) \right\}. \quad (2.1)$$

Let M_λ be the twice-punctured torus

$$M_\lambda = \bar{M}_\lambda \setminus \{(0, 0), (\infty, \infty)\}. \quad (2.2)$$

With the Weierstrass data

$$g(z, w) = z, \quad \eta(z, w) = \frac{dz}{zw}, \quad (2.3)$$

the Weierstrass representation for the Riemann examples \mathcal{R}_λ is

$$R_\lambda(p) := \operatorname{Re} \int_{p_0}^p \Phi_{(g, \eta)} dz, \quad \Phi_{(g, \eta)} := \begin{pmatrix} \frac{(1-z^2)dz}{zw} \\ \frac{i(1+z^2)dz}{zw} \\ \frac{2dz}{w} \end{pmatrix}, \quad p \in M_\lambda. \quad (2.4)$$

The family \mathcal{R}_λ of Riemann examples is parametrized by $\lambda \in (0, \infty)$.

The surface M_λ can be considered to be a double covering of the punctured z -plane, branched at λ and $\frac{-1}{\lambda}$. Consider a circle α in the z -plane with center $\frac{-1}{2\lambda}$ and radius $\frac{1}{2}(\lambda + \frac{1}{\lambda})$, and lift α to a closed curve $\hat{\alpha}$ in M_λ . The Weierstrass integral about $\hat{\alpha}$ results in a nonzero period-vector, and this is the translation T .

Letting $\hat{z} = -z$ and $\hat{w} = iw$, we have

$$\hat{w}^2 = \hat{z}(\hat{z} - \frac{1}{\lambda})(\hat{z} + \lambda).$$

Thus we may consider the map $(z, w) \rightarrow (\hat{z}, \hat{w})$ to be a conformal diffeomorphism between M_λ and $M_{\frac{1}{\lambda}}$.

Because the metric on \mathcal{R}_λ ([Os] p65, [HKR]) is

$$ds^2 = \frac{(1 + |z|^2)^2}{4|z|^2|w|^2} |dz|^2,$$

the maps $(z, w) \rightarrow (\bar{z}, \bar{w})$ and $(z, w) \rightarrow (\bar{z}, -\bar{w})$ both restrict to isometries of M_λ in the induced metric. The set $\mathcal{A} = \{(t, w) \in M_\lambda \mid t \in \mathbb{R}\}$, which consists of the union of their fixed-point sets, is mapped by the Weierstrass integral to geodesics in \mathcal{R}_λ . It is clear from the Weierstrass integral that the intervals in \mathcal{A} of the form $t \leq \frac{-1}{\lambda}$ or $0 < t \leq \lambda$ represent lines in \mathcal{R}_λ , while intervals in \mathcal{A} of the form $\frac{-1}{\lambda} \leq t < 0$ or $t \geq \lambda$ represent planar geodesics in \mathcal{R}_λ . Planar geodesics must be principal curves.

The surfaces \mathcal{R}_λ have the following additional properties:

- 1) \mathcal{R}_λ is foliated by circles and lines in horizontal planes. All the lines in \mathcal{R}_λ are the image under the Weierstrass representation of points in \mathcal{A} such that $t \leq \frac{-1}{\lambda}$ or $0 < t \leq \lambda$, which is the fixed-point set of the map $(z, w(z)) \rightarrow (\bar{z}, -\bar{w}(z))$.
- 2) \mathcal{R}_λ has an infinite number of equally spaced horizontal flat ends. These ends correspond to the punctures of \bar{M}_λ at $z = 0, \infty$.
- 3) \mathcal{R}_λ is invariant under reflection in a plane parallel to the (x_1, x_3) -plane. The intersection of this plane with \mathcal{R}_λ consists of the image under the Weierstrass representation of points in \mathcal{A} such that $\frac{-1}{\lambda} \leq z < 0$ or $z \geq \lambda$, which is the fixed-point set of the map $(z, w(z)) \rightarrow (\bar{z}, \bar{w}(z))$.
- 4) \mathcal{R}_λ is invariant under rotation about horizontal lines that are perpendicular to the (x_1, x_3) -plane, and meet the surface orthogonally at the points where $g(z) = \pm i$. The map $(z, w) \rightarrow (\frac{-1}{z}, \frac{w}{z^2})$ restricted to M_λ represents this rotation.

We will consider a Riemann example to be any surface that is the image of one of these surfaces \mathcal{R}_λ under an isometry or homothety of \mathbb{R}^3 .

2.2 Conjugate Pairs of Riemann Examples

Proposition 2.1 *For any positive $\lambda \neq 1$, the Riemann examples \mathcal{R}_λ and $\mathcal{R}_{\frac{1}{\lambda}}$ are conjugate but not congruent. \mathcal{R}_1 is self-conjugate.*

Proof. Choose $\lambda > 1$. The conjugate surface of \mathcal{R}_λ has Weierstrass data

$$g = z, \\ i\eta = \frac{idz}{zw} = \frac{dz}{(-z)(iw)}.$$

The Weierstrass data for the conjugate surface, expressed in terms of $(\acute{z}, \acute{w}) = (-z, iw)$ on $M_{\frac{1}{\lambda}}$, is

$$\acute{g}(\acute{z}, \acute{w}) = -\acute{z}, \\ \acute{\eta}(\acute{z}, \acute{w}) = \frac{-d\acute{z}}{\acute{z}\acute{w}}.$$

Because

$$\Phi_{(\acute{g}, \acute{\eta})} = \begin{pmatrix} -1 & 0 & 0 \\ 0 & -1 & 0 \\ 0 & 0 & 1 \end{pmatrix} \Phi_{(g, \eta)},$$

it follows from equation (2.4) that the minimal surface in \mathbb{R}^3 with this Weierstrass data is the image of $\mathcal{R}_{\frac{1}{\lambda}}$ under a rotation by π about a vertical axis. Hence \mathcal{R}_λ and $\mathcal{R}_{\frac{1}{\lambda}}$ are conjugate surfaces.

We use the Weierstrass data to show that \mathcal{R}_λ and $\mathcal{R}_{\frac{1}{\lambda}}$ cannot be congruent for $\lambda \neq 1$. Consider the points on \mathcal{R}_λ where $g = \pm 1$. As shown in the previous Section 2.1 (Property 1), when $\lambda > 1$, these points lie on the lines in \mathcal{R}_λ . By contrast, the points of $\mathcal{R}_{\frac{1}{\lambda}}$ where $g(z) = \pm 1$ lie on the planar geodesics in the vertical plane of reflective symmetry of the surface. Suppose there exists a symmetry of \mathbb{R}^3 taking \mathcal{R}_λ to $\mathcal{R}_{\frac{1}{\lambda}}$, then this symmetry must take lines to lines, ends to ends, and planar geodesics to planar geodesics. Since the lines in these two surfaces are all parallel to the x_2 -axis and the ends are horizontal, the symmetry of \mathbb{R}^3 must be of the form

$$\begin{pmatrix} \pm 1 & 0 & 0 \\ 0 & \pm 1 & 0 \\ 0 & 0 & \pm 1 \end{pmatrix}.$$

Therefore points of \mathcal{R}_λ where $g = \pm 1$ must be mapped to points of $\mathcal{R}_{\frac{1}{\lambda}}$ where $g = \pm 1$. This implies that the points of \mathcal{R}_λ and $\mathcal{R}_{\frac{1}{\lambda}}$ where $g = \pm 1$ are the points where the lines and planar geodesics in the surface intersect i.e. where $g = \pm \lambda^{\pm 1}$. But we are assuming $\lambda \neq 1$. Thus \mathcal{R}_λ and $\mathcal{R}_{\frac{1}{\lambda}}$ are not congruent. \square

Remark. One checks that the mapping $(z, w) \rightarrow (z', w')$ from M_λ to $M_{\frac{1}{\lambda}}$ has the property that on fundamental cycles it preserves the periods (one of which is always zero) of (2.4). Hence this mapping induces an isometry of \mathcal{R}_λ and $\mathcal{R}_{\frac{1}{\lambda}}$. \square

Upon considering the behavior of \mathcal{R}_λ and $\mathcal{R}_{\frac{1}{\lambda}}$ as $\lambda \rightarrow 0$, one finds that \mathcal{R}_λ and $\mathcal{R}_{\frac{1}{\lambda}}$ do not have limits that are regular surfaces. However, if these surfaces are normalized appropriately they converge to a catenoid and its conjugate surface, the helicoid, which is consistent with Proposition 2.1. We shall prove this in the next section.

3 Proof of the Main Result

To find a sequence of Riemann examples that converges to a catenoid or helicoid, we renormalize the surfaces \mathcal{R}_λ as follows. Begin the integration in the Weierstrass representation at the point $z_0 = 1$. If $\lambda > 1$, rescale by $\sqrt{\lambda}$; if $\lambda < 1$, rescale by $\frac{1}{\sqrt{\lambda}}$. We name these normalized Riemann examples $\hat{\mathcal{R}}_\lambda$. Note that the rescaling is accomplished by multiplying η in the Weierstrass representation by $\sqrt{\lambda}$ and $\frac{1}{\sqrt{\lambda}}$, respectively. Thus, the Weierstrass representation for $\hat{\mathcal{R}}_\lambda$ is

$$g = z, \eta = \frac{\sqrt{\lambda} dz}{zw}, \lambda \geq 1,$$

$$g = z, \eta = \frac{dz}{\sqrt{\lambda} zw}, \lambda \leq 1.$$

One can check as in Proposition 2.1 that $\hat{\mathcal{R}}_\lambda$ and $\hat{\mathcal{R}}_{\frac{1}{\lambda}}$ are conjugate.

Let K denote Gauss curvature.

Lemma 3.1 *There exists a universal bound c such that $|K| \leq c$ on $\hat{\mathcal{R}}_\lambda$ for all $\lambda \in (0, \infty)$.*

Proof. With Weierstrass data given locally as g and $\eta = f dz$, the Gauss curvature of a minimal surface is ([Os], p76)

$$K = -\left(\frac{4|g'|}{|f|(1+|g|^2)^2}\right)^2. \quad (3.5)$$

In the case of $\hat{\mathcal{R}}_\lambda$ a computation using equations (2.1) and (3.5) yields

$$|K| = 16\lambda^\alpha \frac{|z - \lambda||z + \lambda^{-1}|}{|z|(|z| + |z|^{-1})^4}.$$

where $\alpha = 1$ if $\lambda \leq 1$, and $\alpha = -1$ if $\lambda \geq 1$. If $\lambda \leq 1$, then

$$|K| \leq 16 \frac{(|z| + 1)\lambda(|z| + \lambda^{-1})}{|z|(|z| + |z|^{-1})^4} \leq 16 \frac{(|z| + 1)^2}{|z|(|z| + |z|^{-1})^4} \leq 4.$$

Similarly, if $\lambda \geq 1$, then

$$|K| \leq 16 \frac{\lambda^{-1}(|z| + \lambda)(|z| + 1)}{|z|(|z| + |z|^{-1})^4} \leq 16 \frac{(|z| + 1)^2}{|z|(|z| + |z|^{-1})^4} \leq 4.$$

Thus, $|K|$ has a universal upper bound. □

Remark. More calculation shows that $|K|$ on \mathcal{R}_λ is maximized at a fixed point of one of the symmetries of the surface. Thus K is maximized in one of the following three places: somewhere along a straight line in \mathcal{R}_λ ; somewhere along a planar geodesic in the plane of reflective symmetry parallel to $\{x_2 = 0\}$; or at the points where $g(z) = \pm i$, which are the fixed points of the normal rotation. At the points where $z = g(z) = \pm i$, the value of $|K|$ on \mathcal{R}_λ is $\lambda + \frac{1}{\lambda}$. Hence on $\hat{\mathcal{R}}_\lambda$ the value is $1 + \frac{1}{\lambda^2}$ (resp. $1 + \lambda^2$) when $\lambda > 1$ (resp. when $\lambda < 1$).

The following conjecture has been verified numerically: The absolute value of the Gaussian curvature on \mathcal{R}_λ is maximized at the points where $z = g(z) = \pm i$. This implies that the optimal value in Lemma 3.1 is $c = 2$. \square

Proposition 3.1 *There exist sequences of Riemann examples that converge to a helicoid and sequences that converge to a catenoid.*

Proof. We will prove this proposition by showing that the limit, as $\lambda \rightarrow 0$, of $\hat{\mathcal{R}}_\lambda$ is a catenoid, and the limit, as $\lambda \rightarrow \infty$, of $\hat{\mathcal{R}}_\lambda$ is a helicoid (see Figures 2 through 4). We consider first the case $\lambda \rightarrow 0$.

For a large positive number L , let A_L be the annular ring $\{z \in \mathbb{C} : \frac{1}{L} < |z| < L\}$. One can think of z in (2.1) as a map from M_λ to $\mathbb{C} \setminus \{0\}$. Then for λ sufficiently small, $z^{-1}(A_L)$ consists of two disjoint sets in M_λ . Choose either one and name it $\hat{A}_{L,\lambda}$. Since z parametrizes $\hat{A}_{L,\lambda}$, we shall refer to points in $\hat{A}_{L,\lambda}$ by their z coordinates.

Let B_r be a ball centered at the origin in \mathbb{R}^3 with radius r . Let S_r be the horizontal slab $\{(x_1, x_2, x_3) \in \mathbb{R}^3 \mid -r \leq x_3 \leq r\}$, with boundary planes $x_3 = \pm r$.

Let \mathcal{C} be the catenoid obtained by using the Weierstrass data

$$g(z) = z, \quad \eta(z) = \frac{dz}{z^2},$$

and integrating over $\mathbb{C} \setminus \{0\}$ with base point $z_0 = 1$. The Weierstrass representation for the catenoid \mathcal{C} is

$$C(p) := \operatorname{Re} \int_1^p \begin{pmatrix} \frac{(1-z^2)dz}{z^2} \\ \frac{i(1+z^2)dz}{z^2} \\ \frac{2dz}{z} \end{pmatrix}, \quad p \in \mathbb{C} \setminus \{0\}.$$

Let $\hat{\mathcal{C}}_L$ be the image of the restriction of $C(p)$ to A_L . By examination of the third coordinate of the Weierstrass representation, we see that $\hat{\mathcal{C}}_L = \mathcal{C} \cap S_{2 \ln L}$. Choose a large value for r , and choose $L > e^r$ so that $\mathcal{C} \cap S_{2r} \subseteq \hat{\mathcal{C}}_L$.

For $\lambda < 1$, the Weierstrass representation for $\hat{\mathcal{R}}_\lambda$ is

$$\hat{R}_\lambda(p) := \operatorname{Re} \int_1^p \begin{pmatrix} \frac{(1-z^2)dz}{\sqrt{\lambda}zw} \\ \frac{i(1+z^2)dz}{\sqrt{\lambda}zw} \\ \frac{2dz}{\sqrt{\lambda}w} \end{pmatrix} = C(p) + \operatorname{Re} \int_1^p \begin{pmatrix} f_{0,\lambda}(z) \frac{(1-z^2)dz}{z^2} \\ f_{0,\lambda}(z) \frac{i(1+z^2)dz}{z^2} \\ f_{0,\lambda}(z) \frac{2dz}{z} \end{pmatrix}, \quad (3.6)$$

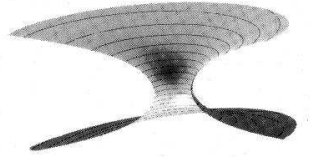


Figure 2: Portion of the Riemann Example \mathcal{R}_λ , $\lambda = 0.1$

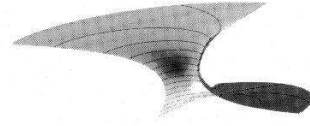


Figure 3: Portion of the Riemann Example \mathcal{R}_λ , $\lambda = 0.5$



Figure 4: Portion of the Riemann Example \mathcal{R}_λ , $\lambda = 1.0$

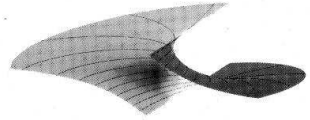


Figure 5: Portion of the Riemann Example \mathcal{R}_λ , $\lambda = 3.0$



Figure 6: Portion of the Riemann Example \mathcal{R}_λ , $\lambda = 5.0$



Figure 7: Portion of the Riemann Example \mathcal{R}_λ , $\lambda = 10.0$

where

$$f_{0,\lambda}(z) = \frac{\sqrt{z}}{\sqrt{(z-\lambda)(\lambda z+1)}} - 1.$$

If λ is close to zero, then the Weierstrass integral \acute{R}_λ along any closed curve in $\acute{A}_{L,\lambda}$ is zero. Therefore the Weierstrass integral depends only on the endpoints of a path in $\acute{A}_{L,\lambda}$. All paths from $z_0 = 1$ to $p \in A_L$ may be chosen to be of length less than cL , where c is some fixed constant.

Note that the functions

$$\frac{1-z^2}{z^2}, \frac{1+z^2}{z^2}, \frac{2}{z}$$

are bounded on A_L . Also, for all $z \in A_L$,

$$\lim_{\lambda \rightarrow 0} |f_{0,\lambda}(z)| = 0.$$

It follows that the last integral in equation (3.6) becomes arbitrarily small, uniformly on $\acute{A}_{L,\lambda}$, as $\lambda \rightarrow 0$. In particular, for all $p \in A_L$, $\lim_{\lambda \rightarrow 0} \acute{R}_\lambda(p) = C(p)$.

Let $\hat{\mathcal{R}}_\lambda$ be the image of $\acute{A}_{L,\lambda}$ under the map $\acute{R}_\lambda(p)$. It follows that $\hat{\mathcal{R}}_\lambda$ is a small perturbation of $\hat{\mathcal{C}}_L$ for λ close to zero. We conclude that $\acute{\mathcal{R}}_\lambda \cap B_r \subseteq \hat{\mathcal{R}}_\lambda$. Thus to examine the behavior of $\acute{\mathcal{R}}_\lambda$, as $\lambda \rightarrow 0$, in arbitrary compact regions of \mathbb{R}^3 , it is enough to examine $\hat{\mathcal{R}}_\lambda$ in B_r for arbitrarily large fixed r .

We claim that the surface $\acute{\mathcal{R}}_\lambda \cap B_r$ is a graph over a subset of the catenoid \mathcal{C} , for λ close to 0. By Lemma 3.1, the Gaussian curvature K is uniformly bounded for all $\acute{\mathcal{R}}_\lambda$. This implies that the normal curvatures are also uniformly bounded. This in turn implies $\acute{\mathcal{R}}_\lambda \cap B_r$ is a union of graphs over a subset of the catenoid \mathcal{C} . Since the surface $\acute{\mathcal{R}}_\lambda$ is foliated by lines and circles in horizontal planes, there is a single graph.

We now show that $\acute{\mathcal{R}}_\lambda \cap B_r$ converges to $\mathcal{C} \cap B_r$, in the C^∞ -topology, as $\lambda \rightarrow 0$. Because the curvature of $\acute{\mathcal{R}}_\lambda$ is bounded uniformly in λ , it follows from standard elliptic theory that the convergence is C^∞ . (Curvature bounds give C^1 estimates.) However, we can give in our specific case a direct proof. Let $p \in \mathcal{C} \cap B_r$. Let $z_p \in A_L$ be the point such that $C(z_p) = p$, and let $B_h(z_p) \subseteq A_L$ be a ball of radius h about z_p . Note that $\acute{R}_\lambda(B_h(z_p))$ consists of disks in \mathbb{R}^3 converging in the C^0 -norm, as $\lambda \rightarrow 0$, to a disk containing p and lying on the catenoid \mathcal{C} . Let $x_{i,\lambda}(z)$ be the i 'th coordinate function of $\acute{\mathcal{R}}_\lambda$, let $x_i(z)$ be the i 'th coordinate function on \mathcal{C} , and let $f_\lambda(z) = x_{i,\lambda}(z) - x_i(z)$. Note that

$$\max_{w \in B_h(z_p)} |f_\lambda(w)| \rightarrow 0, \text{ as } \lambda \rightarrow 0.$$

Since $f_\lambda(z)$ is harmonic, it is the real part of a holomorphic function $F_\lambda(z)$, and $F_\lambda(z)$ can be chosen so that

$$\max_{w \in B_h(z_p)} |F_\lambda(w)| \rightarrow 0, \text{ as } \lambda \rightarrow 0.$$

Assuming $z \in B_{\frac{h}{2}}(z_p)$, and using the Cauchy integral formula, we have

$$\begin{aligned} |f_\lambda^{(k)}(z)| &\leq |F_\lambda^{(k)}(z)| = \left| \frac{k!}{2\pi i} \int_{\partial B_h(z_p)} \frac{F(\xi)}{(\xi - z)^{k+1}} d\xi \right| \\ &\leq \frac{k!}{2\pi} \left(\frac{2}{h} \right)^{k+1} 2\pi h \max_{w \in B_h(z_p)} |F_\lambda(w)|, \end{aligned}$$

and so we have that $|f_\lambda^{(k)}(z)| \rightarrow 0 \forall k, \forall z \in B_{\frac{h}{2}}(z_p)$, as $\lambda \rightarrow 0$. Therefore $|f_\lambda^{(k)}(z)| \rightarrow 0 \forall k, \forall z \in A_L$, and the convergence is in the C^∞ -topology in B_r .

Since r is arbitrary, we have completed the proof that \mathcal{R}_λ converges to the catenoid \mathcal{C} as $\lambda \rightarrow 0$.

It is now intuitively clear that the surfaces \mathcal{R}_λ converge to a helicoid for the following reason: as $\lambda \rightarrow \infty$, their conjugate surfaces $\mathcal{R}_\lambda^\perp$ converge to a catenoid. One can give an explicit proof of this, similar to the proof just given for the case $\lambda \rightarrow 0$. However, there are some differences in the proof of the case $\lambda \rightarrow \infty$. For λ close to ∞ , the representation for \mathcal{R}_λ is

$$\begin{aligned} \hat{R}_\lambda(p) &:= Re \int_1^p \left(\frac{\sqrt{\lambda}(1-z^2)dz}{z^2 w} \right) = \\ &-Re \int_1^p \left(\frac{\frac{i(1-z^2)dz}{z^2}}{\frac{-(1+z^2)dz}{z^2}} \right) + Re \int_1^p \left(\frac{f_{\infty,\lambda}(z) \frac{i(1-z^2)dz}{z^2}}{f_{\infty,\lambda}(z) \frac{-(1+z^2)dz}{z^2}} \right), \end{aligned} \quad (3.7)$$

where

$$f_{\infty,\lambda}(z) = 1 - \frac{\sqrt{z}}{\sqrt{(1 - \frac{z}{\lambda})(z + \frac{1}{\lambda})}}.$$

Note that the first integral in the above sum in equation (3.7) is the Weierstrass integral for a helicoid, since Weierstrass data for a helicoid is

$$g(z) = z, \quad \eta(z) = \frac{idz}{z^2}.$$

If λ is large, then the vertical distance between adjacent planar ends of \mathcal{R}_λ is approximately 2π . This can be verified by integrating the third function in the integrand of the Weierstrass representation from $+1$ to -1 along the half of the unit circle lying in the upper half of the complex plane. This curve is $z = e^{it}, 0 \leq t \leq \pi$. The distance between adjacent planar ends for large λ is

$$Re \int_0^\pi \frac{2\sqrt{\lambda}ie^{it} dt}{\sqrt{e^{it}(e^{it} - \lambda)(e^{it} + \frac{1}{\lambda})}} \approx Re \int_0^\pi \frac{2\sqrt{\lambda}idt}{\sqrt{-\lambda}} = 2\pi.$$

The major difference from the proof in the case $\lambda \rightarrow 0$ is this: When λ is close to ∞ , then a homologically nontrivial loop in $\hat{A}_{L,\lambda}$ has a nonzero real period with respect to the

Weierstrass integral. Now one may only assume that a path from $z = 1$ to $z = p$ in A_L has length less than cnL , where n is the number of times that the path wraps about the origin, and c is some fixed constant. Since the distance between adjacent ends is approximately 2π , it follows that if the wrapping number n about the origin of a path from 1 to p is sufficiently large, then $z = p$ will be mapped by the Weierstrass integral to a point outside B_r . Thus, we may assume there is an upper bound N for $|n|$, depending only on r . Hence, for large λ , we may assume that any path from 1 to p has length less than $\acute{c}L$, where $\acute{c} = cN$.

The other parts of the proof of the case $\lambda \rightarrow \infty$ transfer directly from the proof of the case $\lambda \rightarrow 0$. □

Corollary 3.1 *As $\lambda \rightarrow \infty$, the radius of any level-circle of $\acute{\mathcal{R}}_\lambda$ diverges to infinity.*

Corollary 3.2 *The planar curve described by the set of centers of the horizontal circles that foliate $\acute{\mathcal{R}}_\lambda$ has the property that its maximum curvature approaches zero as $\lambda \rightarrow \infty$.*

It remains to determine what other surfaces are limits of Riemann examples. Three possibilities are clear: a single flat plane; an infinite number of equally-spaced flat planes; and another Riemann example. The following proposition states that these are the only other possibilities, completing the proof of Theorem 1.1.

Proposition 3.2 *Any convergent sequence of Riemann examples converges to one of the following surfaces:*

- a Riemann example;*
- a helicoid;*
- a catenoid;*
- a single flat plane;*
- an infinite number of equally-spaced flat planes.*

Proof. Let $\{\mathcal{R}_j\}_{j=1}^\infty$ be a sequence of Riemann examples converging to a surface \mathcal{S} . From the definition of convergence, \mathcal{S} is clearly minimal, properly embedded, and complete. Without loss of generality we may assume that the limiting normals \vec{v}_j at the ends of the surfaces \mathcal{R}_j converge in \mathbf{S}^2 to a vertical vector. With this normalization, the surfaces \mathcal{R}_j are foliated by circles and lines lying in planes that are becoming horizontal as $j \rightarrow \infty$. These almost-horizontal planes intersect \mathcal{R}_j in connected sets, and these connected sets each consist of a single circle or a single line. Thus every curve $\mathcal{S} \cap \{x_3 = c\}$ is the limit set of a sequence of circles and/or lines. It follows that $\mathcal{S} \cap \{x_3 = c\}$ is either a circle, a line, the empty set or the plane $\{x_3 = c\}$. Recall from the introduction that this implies that each component of \mathcal{S} is either a helicoid, a catenoid, a Riemann example or a plane. Moreover: the helicoid and catenoid must have vertical axes; the plane and the ends of the Riemann example must be horizontal. If \mathcal{S} has more than one component, they must all be horizontal planes (because

\mathcal{S} is fibred by circles or lines, one in each horizontal plane). Suppose \mathcal{S} consists of two or more horizontal planes. Since the points on the surfaces \mathcal{R}_j where the Gauss map is vertical must approach the ends of \mathcal{R}_j as $j \rightarrow \infty$, it is the equally spaced-ends of the surfaces \mathcal{R}_j that converge to \mathcal{S} . Therefore \mathcal{S} is an *infinite* collection of equally-spaced planes. \square

References

- [En] A. Enneper. Die cyklischen Flächen. *Z. Math. u. Phys.* 14, 1869, p393-421.
- [HKR] D. Hoffman, H. Karcher, and H. Rosenberg. Embedded Minimal Annuli in \mathbb{R}^3 Bounded by a Pair of Straight Lines. *Commentarii Mathematici Helvetici*, vol. 66, p599-617, 1991.
- [Ni] Johannes C. C. Nitsche. *Lectures on Minimal Surfaces Vol. 1*. Cambridge University Press, New York, NY, 1989.
- [Os] Robert Osserman. *A Survey of Minimal Surfaces*. Dover Publications, Inc., New York, NY, 1986.
- [Ri] B. Riemann. *Gesammelte mathematische Werke*. 2nd edition, B. G. Teubner, Leipzig, 1892.